

Figure 33: Analysis of Effects of Different Step Size on Convergence Speed of LMS Alogirthm

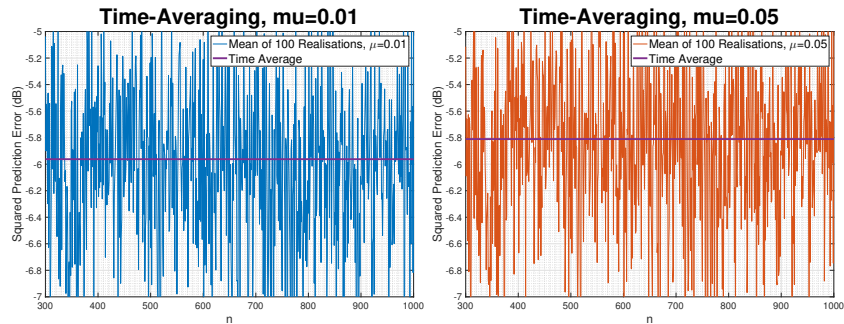


Figure 34: Time-Average of Steady State Error for  $\mu = 0.01$  and  $\mu = 0.05$

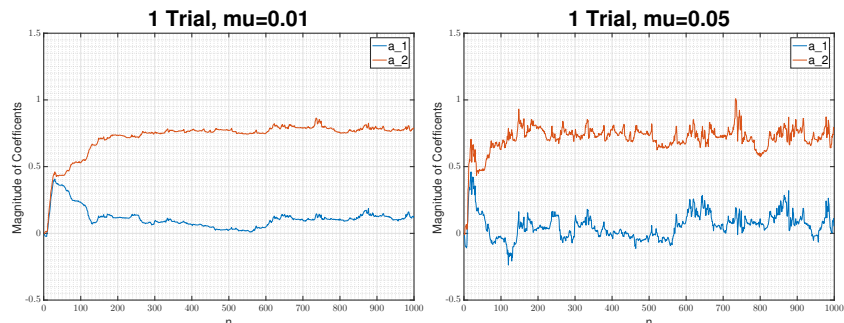


Figure 35: Evolution of Coefficients for 1 Trial, for  $\mu = 0.01$  and  $\mu = 0.05$

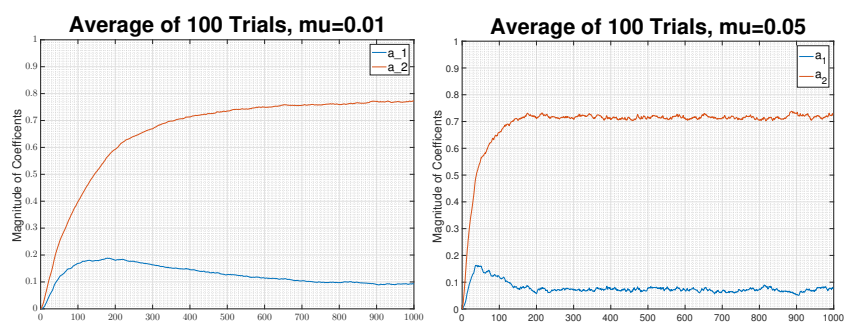


Figure 36: Evolution of Coefficients for 100 Trial, for  $\mu = 0.01$  and  $\mu = 0.05$

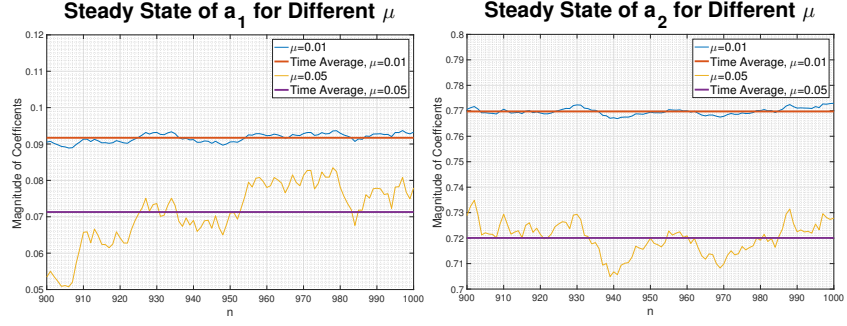


Figure 37: Steady State Values of Coefficients  $a_1$  and  $a_2$ , for  $\mu = 0.01$  and  $\mu = 0.05$

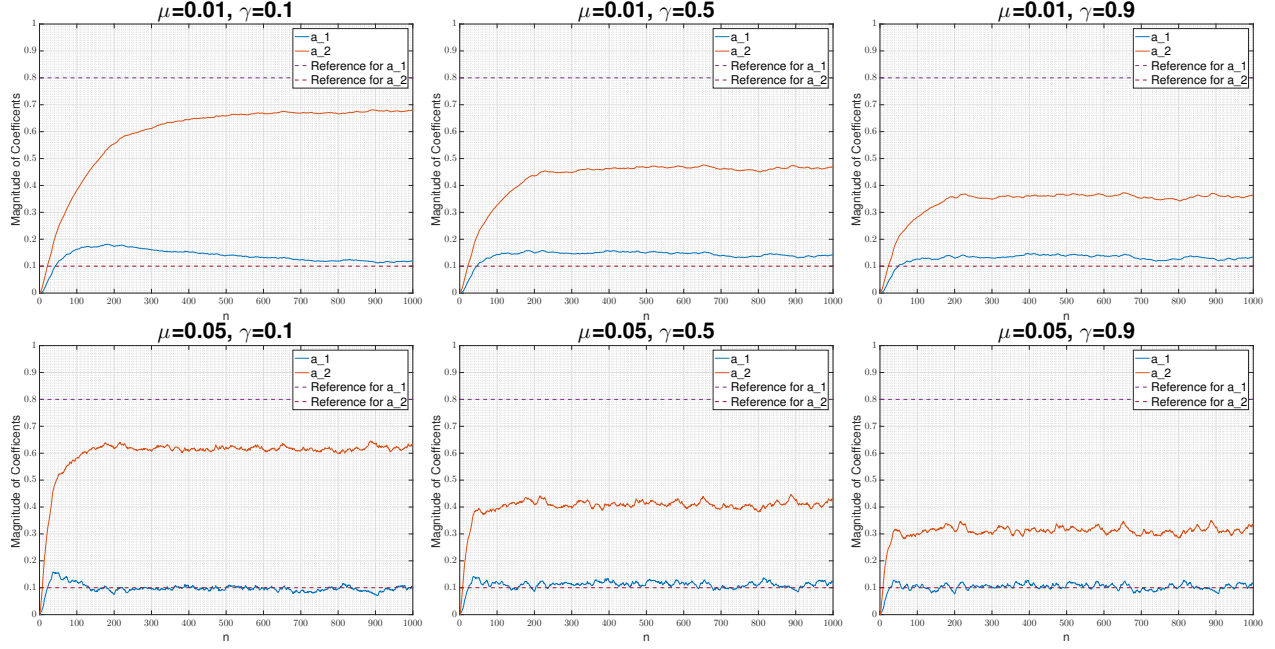


Figure 38: Effect of increasing  $\gamma$  on the Steady State Values of Coefficients  $a_1$  and  $a_2$ , for  $\mu = 0.01$  and  $\mu = 0.05$

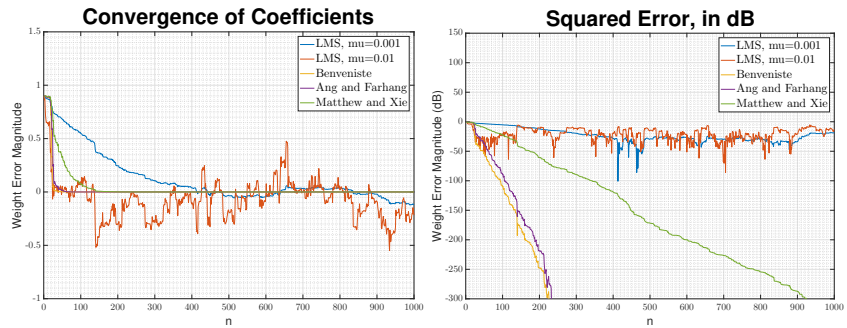


Figure 39: Comparison of Convergence Time using Adaptive Step Sizes and Standard LMS Algorithms

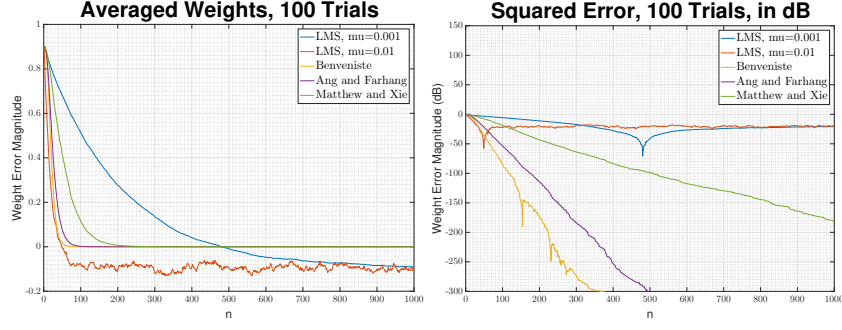


Figure 40: Studying Convergence Time by Averaging Weights over 100 Random Realisations

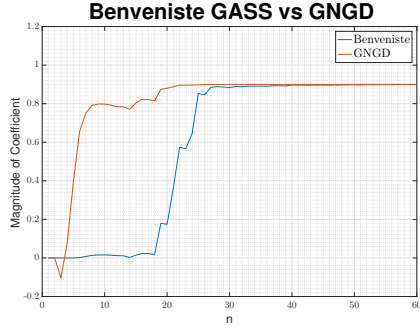


Figure 41: Comparing Convergence Speed of GNGD and Benveniste's GASS Algorithms

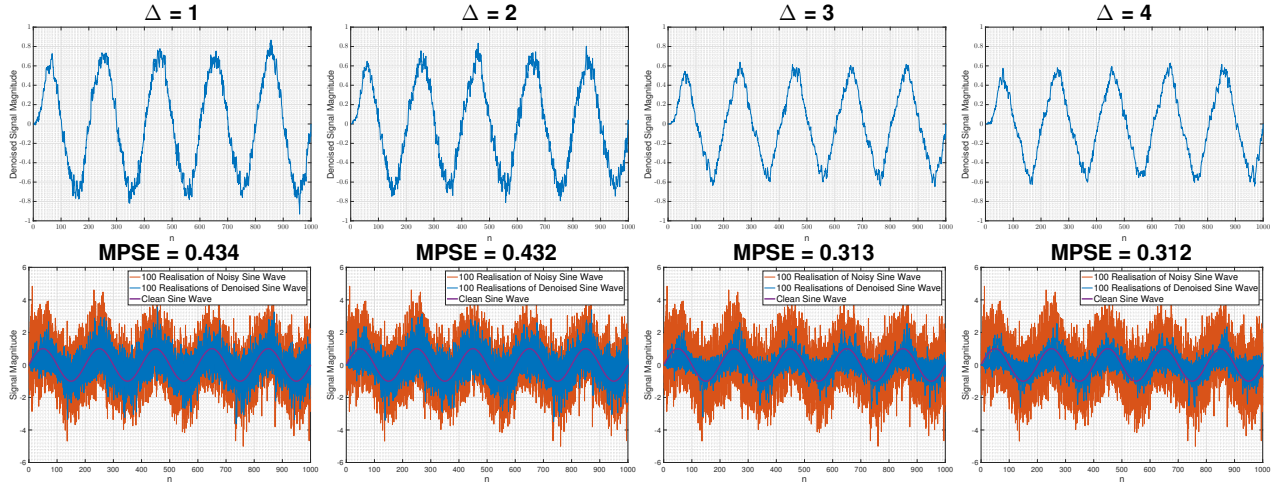


Figure 42: Determining Ideal Value for  $\Delta$  to be used in the Adaptive Line Enhancement Algorithm

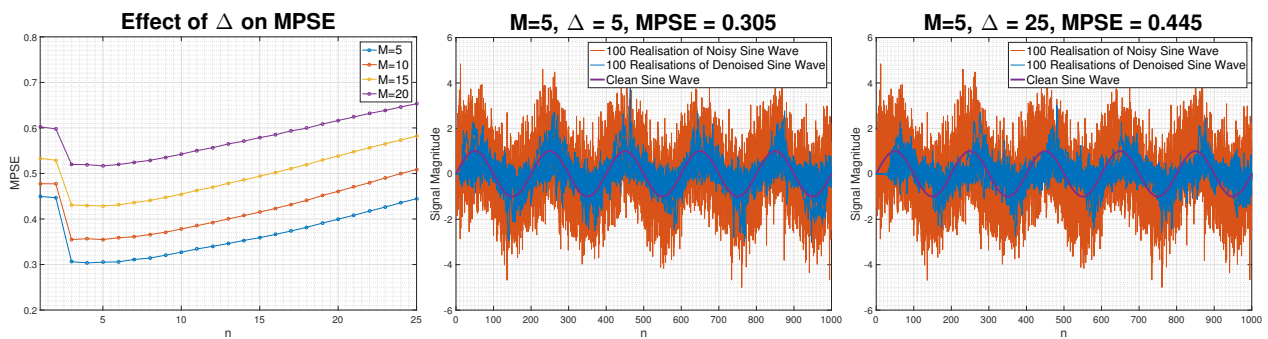


Figure 43: Studying the Effects of Increasing Delay on the MPSE

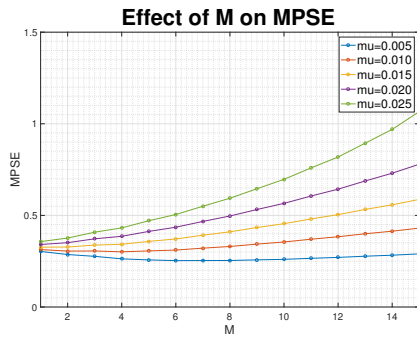


Figure 44: Studying the Effects of Increasing Model Order on the MPSE

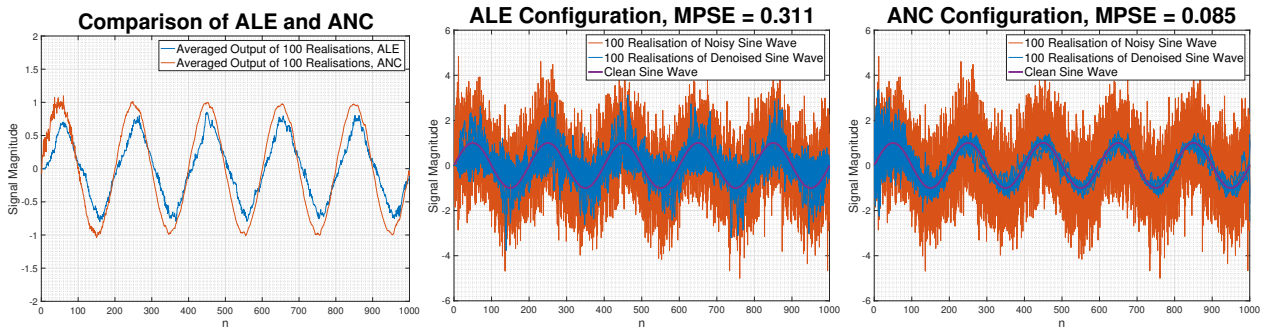


Figure 45: Comparison of ALE and ANC Configurations for Denoising Sinewave

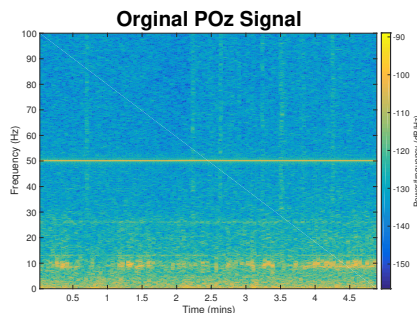


Figure 46: Original EEG Data collected from POz Location on the Scalp with Strong Component at 50 Hz

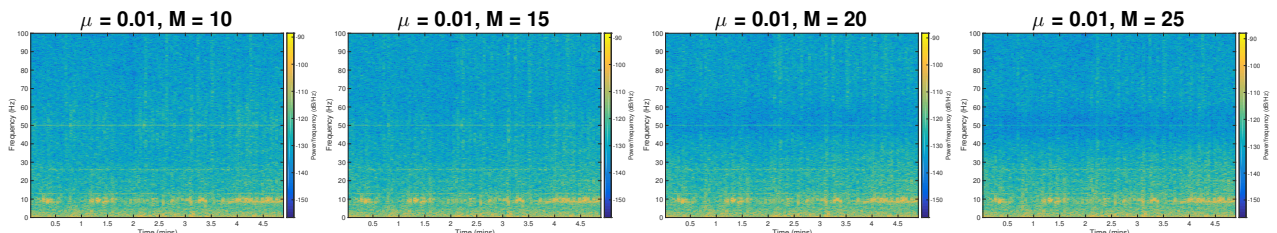


Figure 47: Effect of Increasing Model Order on the Spectrogram of EEG Data

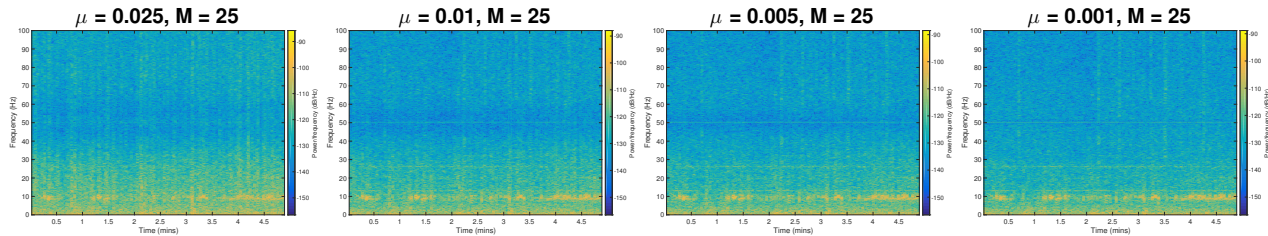


Figure 48: Effect of Varying  $\mu$  on the artifacts observed in the Spectrogram of Denoised EEG Data

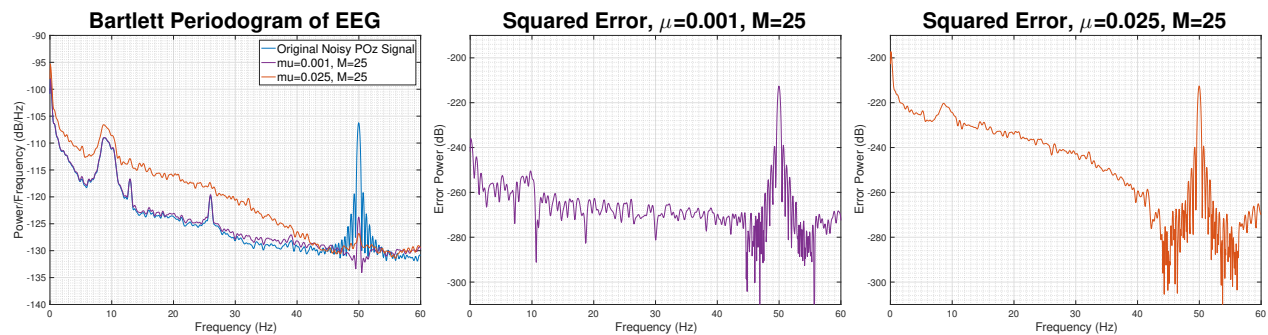


Figure 49: Bartlett Periodogram, averaged over 2 second intervals, and Squared Errors